Investigation of the role of the projectile-target orientation angles on the evaporation residue production

Article *in* Physics of Atomic Nuclei · October 2009

DOI: 10.1134/S1063778809100044

8 authors, including:

Giuseppe Mandaglio
Università degli Studi di Messina

F. Hanappe
Université Libre de Bruxelles

Marina Manganaro
Instituto de Astrofísica de Canarias

A. K. Nasirov
Joint Institute for Nuclear Research

ISSN 1063-7788, Physics of Atomic Nuclei, 2009, Vol. 72, No. 10, pp. 1639–1650. © Pleiades Publishing, Ltd., 2009.

NUCLEI
Experiment

Investigation of the Role of the Projectile–Target Orientation Angles on the Evaporation Residue Production*

G. Mandaglio[1)], G. Fazio[1)], G. Giardina[1)], F. Hanappe[2)], M. Manganaro[1)], A. I. Muminov[3)], A. K. Nasirov[3),4)**], and C. Saccá[5)]

Received December 25, 2008

Abstract—The measured yield of evaporation residues in reactions with massive nuclei have been well reproduced by using the partial fusion and quasifission cross sections obtained in the dinuclear-system model. The influence of the orientation angles of the projectile- and target-nucleus symmetry axes relative to the beam direction on the production of the evaporation residues is investigated for the ^{48}Ca + ^{154}Sm reaction as a function of the beam energy. At the low beam energies only the orientation angles close to $\alpha_P = 30°$ (projectile) and $\alpha_P = 0°–15°$ (target) can contribute to the formation of evaporation residues. At large beam energies (about $E_{\text{c.m.}} = 140–180$ MeV) the collisions at all values of orientation angles α_P and α_T of reactants can contribute to the evaporation residue cross section which ranges between 10–100 mb, while at $E_{\text{c.m.}} > 185$ MeV the evaporation residue cross section ranges between 0.1–1 mb because the fission barrier for the compound nucleus decreases by increasing its excitation energy and angular momentum.

PACS numbers: 25.70.Jj, 25.70.-z
DOI: 10.1134/S1063778809100044

INTRODUCTION

The study of the role of the entrance channel dynamics in the formation of the evaporation residues (ER) in reactions with massive nuclei is an actual problem in establishing the conditions to obtain new superheavy elements or new isotopes far from the iceland of stability of chemical elements. The main requirements to reach maximal cross sections in the formation of the evaporation residues are as small as possible values of the excitation energy and angular momentum of the being formed compound nucleus with large fusion probability. In the cold fusion reactions the main requirements have been satisfied and $1n$ and $2n$ reactions (by emission of one or two neutrons from the compound nucleus) led to observation events confirming the synthesis of superheavy elements $Z = 110$ [1], 111, and 112 (see [1, 2]), as well as element $Z = 113$ (see [2, 3]). The events proving the synthesis of more heavy new elements $Z =$ 114, 115, 116, 118 were observed in the hot fusion reactions with ^{48}Ca on the actinide targets ^{244}Pu, ^{243}Am, ^{248}Cm, and ^{249}Cf, respectively, in which the excitation energy of the compound nucleus was more than 35 MeV [3]. There is an opinion that the values of beam energy leading to the observed maximal cross sections of evaporation residues correspond to the equatorial collisions of the deformed actinide targets (the orientation angle of the nucleus symmetry axis to the beam direction is 90° [4]). The results of our calculations showed that the maximal cross sections should be observed at orientation angles less than 90° because of influence of the entrance channel on the dynamics of capture [5]. Therefore, to investigate the evaporation residue production, it is important to analyze the role of the entrance channel characteristics as the beam energy, orbital angular momentum, orientation angles of the symmetry axes of the projectile and target nuclei relative to the beam direction in the angular momentum distribution of the excited compound nucleus. Although the reaction cross section for the interaction of massive nuclei is large enough, only very small part ($\sigma_{\text{ER}}/\sigma_{\text{react}} \sim 10^{-8}$ or lower) can belong to the expected evaporation residue events at synthesis of superheavy elements $Z > 108$ [1–3]. In fact, the complete fusion of two massive nuclei is in competition with the quasifission (QF) process.

---

*The text was submitted by the authors in English.

[1)]INFN, Sezione di Catania, and Dipartimento di Fisica dell'Universitá di Messina, Italy.
[2)]Université Libre de Bruxelles, Belgium.
[3)]Department of Heavy Ion Physics, Institute of Nuclear Physics, Uzbekistan Academy of Sciences, Tashkent, Uzbekistan.
[4)]Joint Institute for Nuclear Research, Dubna, Russia.
[5)]Dipartimento di Scienze della Terra dell'Universitá di Messina, Italy.
[**]E-mail: nasirov@jinr.ru

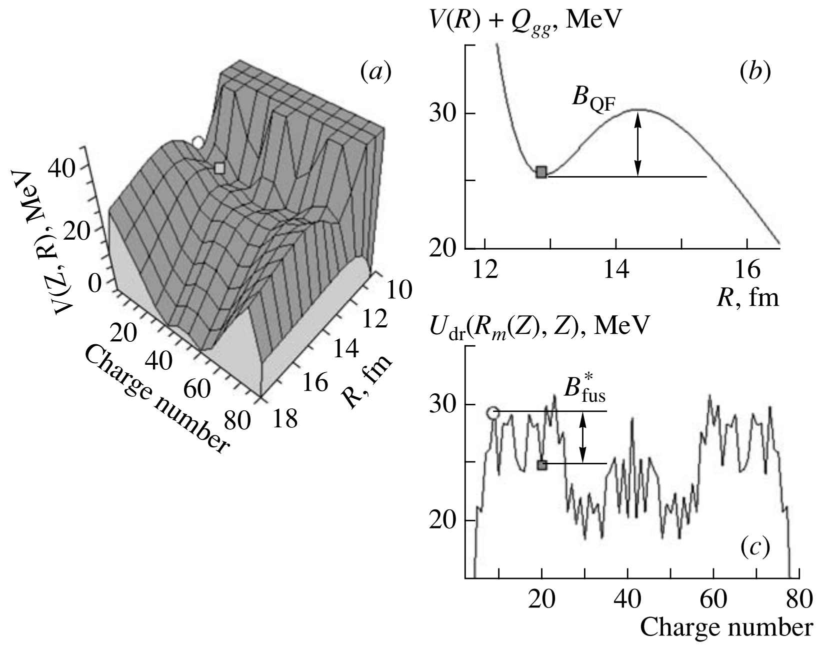

Fig. 1. (a) Potential energy surface for the ^{48}Ca + ^{154}Sm reaction leading to ^{202}Pb as a function of the charge asymmetry of the dinuclear system fragments and the relative distance between their centers. (b) The nucleus–nucleus interaction potential $V(R)$ for the ^{48}Ca + ^{154}Sm system shifted on the reaction Q_{gg} value: the quasifission barrier $B_{\rm QF}$ as the depth of the potential well. (c) Driving potential for the ^{48}Ca + ^{154}Sm reaction as a function of the charge asymmetry of the dinuclear system fragments: the intrinsic fusion barrier $B^*_{\rm fus}$ is shown as the difference between the maximum value of the driving potential to the way of complete fusion and its value corresponding to the considered charge asymmetry of the entrance channel.

The latter process is reseparation of the intermediate dinuclear system into two fragments without reaching of the compound nucleus stage during its evolution after the first capture -stage of the reaction. If the heated and rotating compound nucleus is formed by the alternative way against quasifission channel the evaporation process (leading to the evaporation residue nuclei) takes place which competes with the fission of the compound nucleus and other intermediate nuclei along the deexcitation cascade of compound nucleus. It is well known that the fission barrier for a compound nucleus decreases by increasing its angular momentum and disappears at the definite value ℓ_f [6]. In this case dinuclear system (DNS) being transformed into compound nucleus does not reach an equilibrium state of compact shape and it exists for short time in the nonequilibrium state of the fast rotating mononucleus. Therefore, the mononucleus having high values of the angular momentum, splits into two fragments immediately if its angular momentum is larger than ℓ_f, because there is no barrier providing stability. This process is called the fast fission with formation of binary fragments. So it is a disintegration into two fragments of the mononucleus which has survived against quasifission.

In this paper we present the results of our study showing how the orientation angles of the symmetry axes of the projectile and target nuclei relative to the beam direction and orbital angular momentum affect the yields of the evaporation residues. We analyze the experimental data of the evaporation residue cross sections presented in [7] for the ^{48}Ca + ^{154}Sm reaction because fission probability of the compound nucleus ^{202}Pb is small, consequently, complete fusion and evaporation residues cross sections are nearly equal at relatively low excitation energies.

1. METHOD

We use the method developed in our previous papers [6–9] to describe the role of the full three stages starting from the DNS formation [10] at capture of the projectile by the target nucleus, then its evolution into a compound nucleus and the production of the evaporation residues after emission of γ quanta, neutrons, protons, α particles. The method allows us to determine the corresponding cross sections of capture, complete fusion, and formation of the evaporation residues. By this method we are able to determine the angular momentum distribution of the cross section at the stage of the DNS formation (determined by the conditions of the entrance channel) and the competition between quasifission and complete fusion affected by the conditions of the reaction mechanism. Therefore, also the deexcitation chain of the compound nucleus (characterized by the fission–evaporation competition) is affected by the reaction dynamics [11, 12].

We should remind the strong difference between fusion mechanism of light and massive nuclear systems: for the former system capture and fusion cross sections are nearly equal, while for the latter system there is a hindrance to fusion. This hindrance is competition between complete fusion and quasifission.

In Fig. 1, we presented potential energy surface (PES) calculated for the $^{48}\mathrm{Ca}+{}^{154}\mathrm{Sm}$ reaction leading to $^{202}\mathrm{Pb}$. The probability of fusion is determined by both the collision energy of nuclei and the relief of PES of the DNS calculated as a function of the relative distance and mass asymmetry (Fig. 1a). The curve in Fig. 1b is the sum of the nucleus–nucleus potential and reaction Q_{gg}-value calculated for the $^{48}\mathrm{Ca}+{}^{154}\mathrm{Sm}$ reaction. In our model, the depth of the potential well is used as the quasifission barrier B_{QF} for the given charge asymmetry. In Fig. 1c, the curve connecting minima of the valley on the PES is the driving potential (U_{dr}) as a function of the charge asymmetry of the DNS fragments. The cut of PES for the given charge number is the nucleus–nucleus interaction potential $V(R)$. For the interacting deformed nuclei PES depends on the orientation angles of the symmetry axes and it is calculated by formula:

$$U(Z,A,R,\{\beta_i^{(k)}\},\{\alpha_k\}) = Q_{gg} - V_{\mathrm{rot}}^{(\mathrm{CN})}(\ell) \quad (1)$$
$$+ V(R,Z,Z_{\mathrm{CN}}-Z;\{\beta_i^{(k)}\},\{\alpha_k\})$$
$$+ V_{\mathrm{rot}}^{(\mathrm{DNS})}(\ell,\{\beta_i^{(k)}\},\{\alpha_k\}),$$

where $Q_{gg}=B_1(Z)+B_2(Z_{\mathrm{CN}}-Z)-B_{\mathrm{CN}}(Z_{\mathrm{CN}})$, B_1, B_2, and B_{CN} are binding energies of the constituent nuclei of DNS and compound nucleus, respectively; $Z_{\mathrm{CN}}=Z_1+Z_2$, Z_1 and Z_2 are charge numbers of the projectile and target nuclei, respectively; $V(R,Z,Z_{\mathrm{CN}}-Z)$ is the nucleus–nucleus interaction potential of the DNS nuclei; $V_{\mathrm{rot}}^{(\mathrm{DNS})}(\ell)$ and $V_{\mathrm{rot}}^{(\mathrm{CN})}(\ell)$ are rotational energies of DNS and the compound nucleus. $\beta_i^{(1,2)}$ and $\alpha_{1,2}$ are deformation parameters and orientation angles of axial symmetry axis of interacting nuclei. The binding energy values are obtained from the tables in [13, 14].

The cross section of evaporation residues, which can be compared with the corresponding experimental data, is calculated by the determination of the survived $^{A_{\mathrm{CN}}}Z_{\mathrm{CN}}$ compound nucleus and other excited intermediate nuclei along the deexcitation cascade after emission of ν neutrons, y protons, k α-particles at the xth step of the cascade by the formula [11, 15]:

$$\sigma_{\mathrm{ER}(x)}(E_x^*) \quad (2)$$
$$= \sum_{\ell=0}^{\ell_f}(2\ell+1)\sigma_{(x-1)}^{\ell}(E_x^*)W_{\mathrm{sur}(x-1)}(E_x^*,\ell),$$

where $\sigma_{(x-1)}^{\ell}(E_x^*)$ is the partial cross section of the intermediate nucleus formation at the $(x-1)$th step, and $W_{\mathrm{sur}(x-1)}(E_x^*,\ell)$ is the survival probability of the $(x-1)$th intermediate nucleus against fission along the deexcitation cascade of compaund nuclei; E_x^* is an excitation energy of the nucleus at the xth step of the deexcitation cascade. It is clear that $\sigma_{(0)}^{\ell}(E_{\mathrm{CN}}^*)$ is equal to the cross section of compound nucleus formation $\sigma_{\mathrm{fus}}^{\ell}(E_{\mathrm{CN}}^*)$ with excitation energy

$$E_{\mathrm{CN}}^* = E_{\mathrm{c.m.}} + Q_{gg} - V_{\mathrm{rot}}^{(\mathrm{CN})}(\ell), \quad (3)$$

where $E_{\mathrm{c.m.}}$ is the collision energy in the center-of-mass system. The numbers of the being emitted neutrons, protons, α-particles and γ-quanta, $\nu(x)n$, $y(x)p$, $k(x)\alpha$, and $s(x)\gamma$, respectively, are functions of excitation energy at the step x. The emission branching ratios of these particles depend on the excitation energy E_x^* and angular momentum ℓ_x of the being cooled intermediate nucleus.

In our model, we calculate $\sigma_{\mathrm{fus}}^{\ell}(E_{\mathrm{CN}}^*)$ by estimation of the competition of the complete fusion with quasifission if we can calculate the partial capture cross section:

$$\sigma_{\mathrm{fus}}^{\ell}(E_{\mathrm{c.m.}}) = \sigma_{\mathrm{cap}}^{\ell}(E_{\mathrm{c.m.}})P_{\mathrm{CN}}(E_{\mathrm{c.m.}},\ell), \quad (4)$$

where $P_{\mathrm{CN}}(E_{\mathrm{c.m.}})$ is the fusion probability for formation of the compound nucleus during evolution of the DNS at presence of the competition between complete fusion and quasifission. Details of the method to calculate $\sigma_{\mathrm{cap}}^{\ell}$ and $\sigma_{\mathrm{fus}}^{\ell}$ are described in [5, 15].

The partial capture cross section at given beam energy $E_{\mathrm{c.m.}}$ and orbital angular momentum ℓ is determined by the formula

$$\sigma_{\mathrm{cap}}^{\ell}(E_{\mathrm{c.m.}}) = \pi\lambda\!\!\!^{-}{}^2\mathcal{P}_{\mathrm{cap}}^{\ell}(E_{\mathrm{c.m.}}), \quad (5)$$

where $\mathcal{P}_{\mathrm{cap}}^{\ell}(E_{\mathrm{c.m.}})$ is the capture probability which is equal to 1 or 0 for the given beam energy and orbital angular momentum in dependence on the colliding nuclei trapped or not trapped into the well of the nucleus–nucleus potential after dissipation of a part of the initial kinetic energy and orbital angular momentum. Our calculations showed that in dependence on the collision energy $E=E_{\mathrm{c.m.}}$, a window for the orbital angular momentum leading to capture can be a function of the orbital angular momentum [5]:

$$\mathcal{P}^{\ell}_{\rm cap}(E) = \begin{cases} 1, & \text{if} \quad \ell_{\min} \le \ell \le \ell_d \quad \text{and} \quad E > V_{\rm Coul}, \\ 0, & \text{if} \quad \ell < \ell_{\min} \quad \text{or} \quad \ell > \ell_d \\ & \text{and} \quad E > V_{\rm Coul}, \\ 0, & \text{for all} \quad \ell \qquad \text{if} \quad E \le V_{\rm Coul}. \end{cases}$$

The boundary values $\ell_{\min}$ and ℓ_d of the partial waves leading to capture depend on the dynamics of collision and they are determined by solving the equations of motion for the relative distance R and orbital angular momentum ℓ [8, 16, 17]. At lower beam energies $\ell_{\min}$ goes down to zero and we do not observe the ℓ "window": $0 \le \ell \le \ell_d$. They are defined by the size of the potential well of the nucleus–nucleus potential $V(R, Z_1, Z_2)$ and the values of the radial γ_R and tangential γ_t friction coefficients, as well as by the moment of inertia for the relative motion [5, 8]. The capture cross section is determined by the number of partial waves that lead colliding nuclei to trap into the well of the nucleus–nucleus potential after dissipation of the sufficient part of the initial kinetic energy (see, for example Fig. 1*a* of [5, 8]). The size of the potential well decreases by increasing the orbital angular momentum ℓ. The value of ℓ at which the potential well disappears is defined as the critical value $\ell_{\rm cr}$.

Due to the dependence of the nucleus–nucleus potential $V(R)$ and moment of inertia (J_R) for DNS on the orientations of the axial symmetry of deformed nuclei, the excitation functions of the capture and fusion are sensitive to the orientation angles under discussion. This was demonstrated in [5, 18]. The present paper is devoted to the study of the dependence of the evaporation residue cross section on the orientation angles of the deformed nuclei. Certainly, it is impossible to establish directly the abovementioned dependence in an experimental way. But the theoretical analysis allows us to estimate the contributions of collisions by different orientation angles to the measured evaporation residue cross sections. Conclusions of such kind of analysis are useful to find favorable values of the beam energy for the synthesis of superheavy elements in reactions with deformed nuclei.

Usually, the final results of the evaporation residue cross sections are obtained by averaging the contributions calculated for the different orientation angles of the symmetry axis of the reacting nuclei:

$$\langle \sigma_{ER}(E_{\rm c.m.})\rangle = \int_0^{\pi/2} \sin\alpha_P \int_0^{\pi/2} \sigma_{\rm ER}(E_{\rm c.m.}; \alpha_P, \alpha_T) \sin\alpha_T d\alpha_P d\alpha_T, \tag{6}$$

where $\sigma_{\rm ER}(E_{\rm c.m.}; \alpha_P, \alpha_T)$ is calculated by formula (2) for all considered orientation angles of the symmetry axes of the projectile and target nuclei. The fusion excitation function is determined by product of the partial capture cross sections $\sigma^{\ell}_{\rm cap}$ and fusion probabilities $P_{\rm CN}$ of DNS:

$$\sigma_{\rm fus}(E; \alpha_P, \alpha_T) = \sum_{\ell=0}^{\ell_f} (2\ell+1)\sigma_{\rm cap}(E, \ell; \alpha_P, \alpha_T) P_{\rm CN}(E, \ell; \alpha_P, \alpha_T), \tag{7}$$

while the quasifission cross section is defined by

$$\sigma_{\rm QF}(E; \alpha_P, \alpha_T) = \sum_{\ell=0}^{\ell_d} (2\ell+1) \times \sigma_{\rm cap}(E, \ell; \alpha_P, \alpha_T)(1 - P_{\rm CN}(E, \ell; \alpha_P, \alpha_T)), \tag{8}$$

where the capture cross section includes all events with the full momentum transfer as complete fusion, quasifission, and fast fission cross sections:

$$\sigma^{\ell}_{\rm cap}(E) = \sigma^{\ell}_{\rm fus}(E) + \sigma^{\ell}_{\rm QF}(E) + \sigma^{\ell}_{\rm fast\ fiss}(E). \tag{9}$$

Here,

$$\sigma^{\ell}_{\rm fus}(E) = \sigma^{\ell}_{\rm ER}(E) + \sigma^{\ell}_{\rm fiss}(E). \tag{10}$$

The fission cross section of compound nucleus with the excitation energy $E^*_{\rm CN}$ and angular momentum $\ell_{\rm CN}$ is calculated by the advanced statistical code [15, 19, 20] that takes into account the damping of the shell correction in the fission barrier as a function of the nuclear temperature and orbital angular momentum. Memory from the entrance channel is pronounced in the angular momentum distribution of the heated and rotating compound nucleus $\sigma_{\rm fus}(E^*_{\rm CN}, \ell_{\rm CN}; \alpha_P, \alpha_T)$ which depends on the orientation angles α_P and α_T of the symmetry axes of the reactant nuclei.

2. RESULTS AND DISCUSSION

To investigate the influence of the orientation angles of the projectile and target nuclei on the evaporation residue yields, we choose the ^{48}Ca + ^{154}Sm reaction because fission probability of the compound nucleus ^{202}Pb is small and, therefore, at not so large beam energies complete fusion cross section is nearly equal to the evaporation residue cross section according to formula (5). The experimental data of the

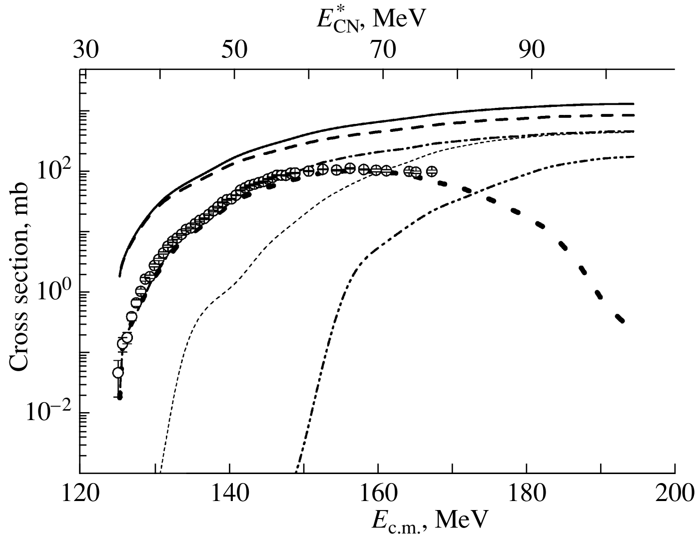

Fig. 2. The theoretical excitation functions for capture (solid curve), fusion + fast fission (dash-dotted curve), quasifission (dashed line), evaporation residue (thick short-dashed curve), the fusion–fission (thin short-dashed curve) and fast fission (dash-double-dotted curve) versus the beam energy $E_{\rm c.m.}$ for the ^{48}Ca + ^{154}Sm reaction leading to the ^{202}Pb compound nucleus. Open circles are the experimental data of the evaporation residues given in [20].

evaporation residue cross sections measured in detail for this reaction are presented in [7]. To understand in detail the preceding mechanism leading to the formation of the evaporation residues we study the dependence of the competition between quasifission and complete fusion on the orientation angles α_P and α_T of the symmetry axes of the projectile and target nuclei, respectively. The quadrupole deformation parameter of ^{154}Sm is equal to 0.27 in the ground state. Although ^{48}Ca is spherical, calculation of fusion cross section considering ^{48}Ca as a spherical nucleus does not allow us to describe the low-energy part of the experimental excitation function of evaporation residues. Therefore, in our calculations we take into account the quadrupole 2^+ and octupole 3^- collective excitations and we used for it the value ($\langle\beta_2^{(+)}\rangle = 0.101$) (from [21]) and $\langle\beta_3^{(-)}\rangle = 0.25$ (from [22]) as the effective deformation parameters. We stress the good agreement between our results for evaporation residues and the experimental data of [7] (see Fig. 2). The evaporation residue data are comparable with the fusion cross section at the beam energies lower than $E_{\rm c.m.} = 150$ MeV while at the beam energies higher than $E_{\rm c.m.} = 160$ MeV the fission cross section becomes larger than the evaporation residues becoming comparable with the fusion cross section. Theoretical results for evaporation residues data were obtained by the use of formula (6).

At energies $E_{\rm c.m.} = 140$–180 MeV, collisions with all orientation angles contribute to the evaporation residue formation and the evaporation residue cross section ranges between 10–100 mb, while at $E_{\rm c.m.} >$ 185 MeV the formation probability of the evaporation residues decreases and $\sigma_{\rm ER}$ ranges between 0.1–1 mb. The decrease of evaporation residues is explained by a decrease in the fission barrier B_f of the compound nucleus (CN), which is caused by an increase in its excitation energy and angular momentum [11]. The angular momentum distribution of the heated and rotating CN (and other intermediate nuclei along the deexcitation cascade of CN) plays a decisive role in the formation of evaporation residues and is taken into account in our calculation of CN survival probability againts fission [11].

At energies lower than about $E_{\rm c.m.} = 140$ MeV, the quasifission contribution is comparable with the capture formation, and the fusion process is strongly hindered. Because at low energies only the small orientation angles of the symmetry axis of the projectile–target nuclei relative to the beam direction give appreciable contributions to the fusion cross section (see, for example, in Fig. 3 the configurations near to about $\alpha_P = 30°$ and $\alpha_T = 15°$). Calculations of the driving potential $U_{\rm dr}$ show that the hindrance to complete fusion is larger for collisions with small values of α_P and α_T. The hindrance factor is connected with the intrinsic fusion barrier $B^*_{\rm fus}$ which is a function of α_P and α_T (see Fig. 4). This is connected with the dependence of PES, particularly of the driving potential $U_{\rm dr}$, on the orientation angles (see Fig. 4). As a result, the competition between complete fusion and quasifission becomes a function of α_P and α_T (see [15]). In this model, $B^*_{\rm fus}$ is determined as a difference of the value of the driving potential which

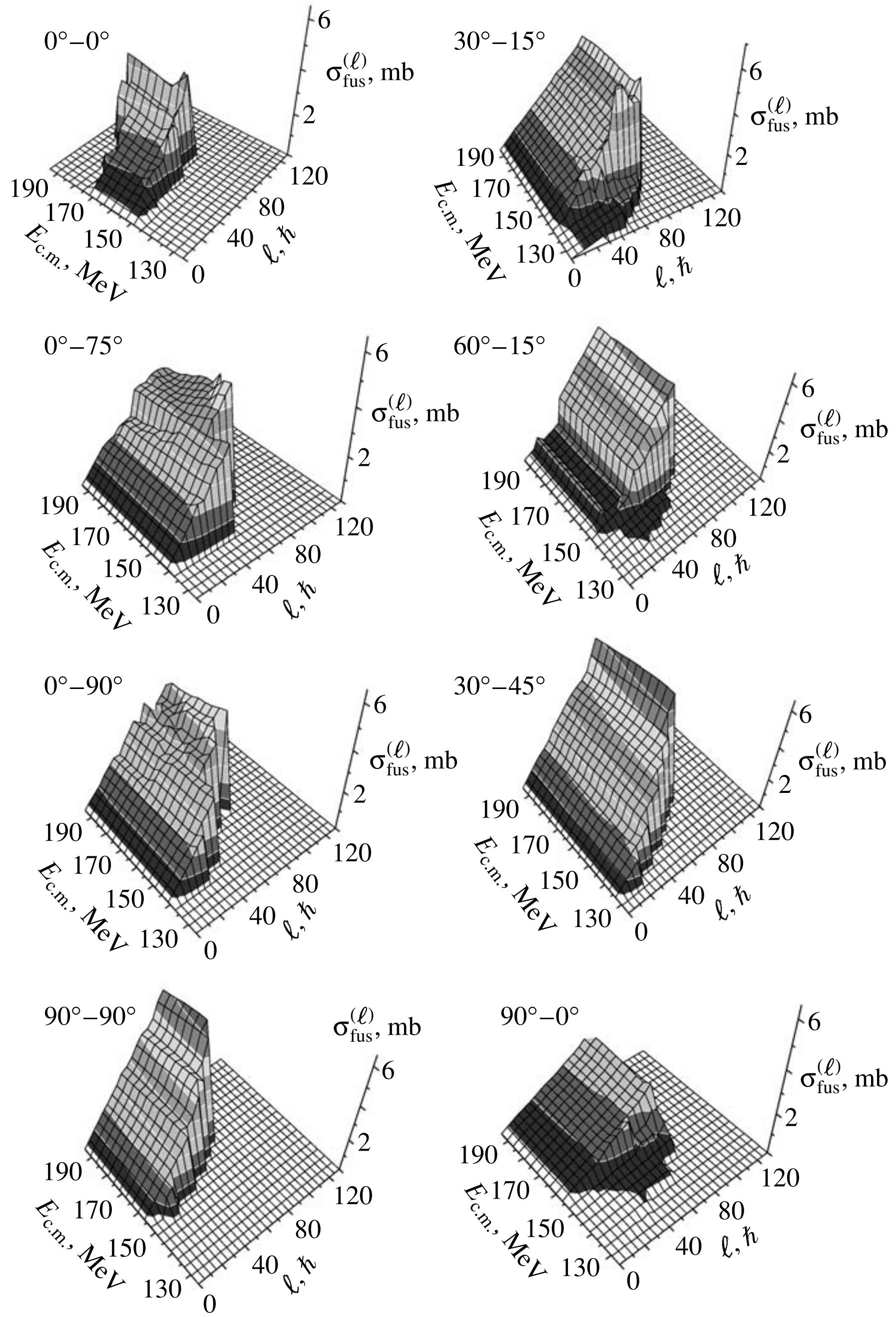

Fig. 3. Spin distribution of the fusion cross section as a function of $E_{\rm c.m.}$ and ℓ, at various α_P–α_T orientation angles of the reacting nuclei.

corresponds to the initial mass asymmetry (its value is marked by square in Figs. 1a and 4) and its maximum value (the point marked by a circle in Figs. 1a and 4). One can see in Fig. 4 that the intrinsic fusion barrier $B^*_{\rm fus}$ decreases by the increase of α_P and α_T. As a result, the fusion probability $P_{\rm CN}$ increases. The values of $B^*_{\rm fus}$ are larger for the small orientation angles of the symmetry axes relative to the beam direction in comparison with that for the large orientation angles.

Figure 3 shows the angular momentum distribution of the compound nucleus as a function of the beam energy $E_{\rm c.m.}$ for some orientation angles of the symmetry axes of the projectile–target nuclei. The volumes of distributions strongly depend on the orientation angles α_P–α_T of reactants. This figure shows that the orientation angles close to $\alpha_P = 30°$ and $\alpha_T = 15°$ can only give the main contribution to the complete fusion at beam energies lower than about $E_{\rm c.m.} = 130$ MeV because for these orienta-

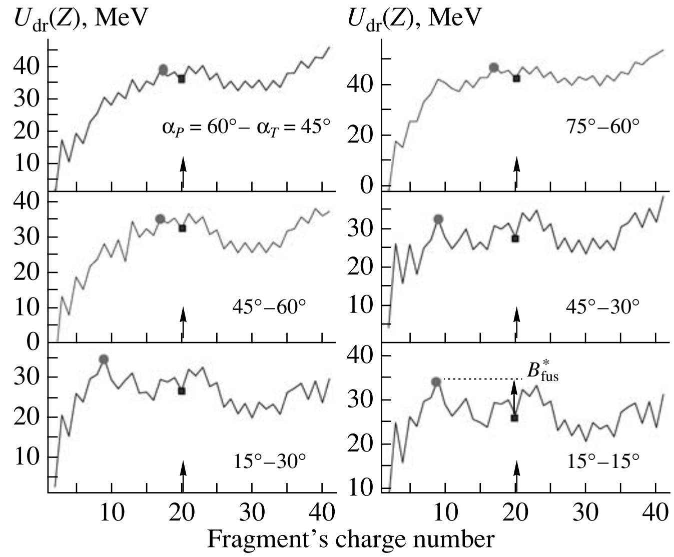

Fig. 4. The dependence of the driving potential and intrinsic barrier B^*_{fus} (for $\ell = 0$) on the orientation angles of the projectile (α_P) and target (α_T) nuclei for the ^{48}Ca + ^{154}Sm reaction.

tions the Coulomb barrier is low. At larger values of the beam energy, the number of the orientations which give contributions to the complete fusion increases.

It is seen that at small values of $E_{\text{c.m.}}$ the partial fusion cross sections are small at tip–tip collision ($\alpha_P = 0°$ and $\alpha_T = 0°$) due to strong competition with quasifission channel. The dominant role of the quasifission in reactions with massive deformed nuclei at low energies was discussed in the paper by Hinde *et al.* [23] showing the increase of the anisotropy of the fragment angular distribution at the lowest beam energies in the ^{16}O + ^{238}U reaction. This phenomenon connected with the contribution of quasifission in the observed anisotropy of the fragment angular distribution was explored in [18] in the framework of the model based on the dinuclear-system concept [24]: competition (P_{CN}) between complete fusion and quasifission is determined by the ratio of level densities on the maximum of the PES (marked by circle) taken as a function of a fragment's charge number (Fig. 4).

The increase of the angular momentum ℓ of the compound nucleus by the increase of the beam energy is a common phenomenon for the collisions of all orientation angles. As it was mentioned above, that if angular momentum of the DNS being fused is larger than ℓ_f, when there is no barrier providing stability of compound nucleus, the system undergoes fast fission with formation of binary fragments. The difference between fast fission and quasifission processes is that for the former the necessary and sufficient conditions for complete fusion are satisfied but the condition of stability of compound system is not satisfied, while for latter process even the sufficient condition of fusion is not satisfied. The binary fragments of these processes can be recognized by their angular distributions: the angular distribution of the fast fission products expected to be less asymmetric than one of quasifission products. The lifetime of DNS leading to fast fission is longer and its angular momentum is usually large ($\ell_{\text{DNS}} > \ell_f$) according to definition of fast fission. So fast fission is a disintegration of the mononucleus into two fragments which has survived against quasifission. We remind that the compound nucleus is not formed in both cases. The cross section of the fast fission events is shown by dash-double-dotted curve in Fig. 2. So the fast fission cross section becomes appreciable at the collision energies higher than $E_{\text{c.m.}} = 160$ MeV, while the evaporation residue cross section strongly decreases. The decrease of the evaporation residue yield is explained by increase of the excitation energy and angular momentum of compound nucleus ^{202}Pb formed at complete fusion in ^{48}Ca + ^{154}Sm reaction. The dependence of the angular momentum distribution of compound nucleus on the orientation angles of colliding nuclei is presented in Fig. 3. Moreover, the figure also shows a completely different shape of the volume and features between the 90°–0° and 0°–90° angular configurations of reacting nuclei, because the used deformation parameters are different for the projectile ($\langle\beta_2^{(2+)}\rangle = 0.101$) and target ($\langle\beta_2^{(2+)}\rangle = 0.270$).

The large and extended distribution of the partial cross section for the orientation angles $\alpha_P = 30°$ and $\alpha_T = 45°$ is caused by wide and deep potential well.

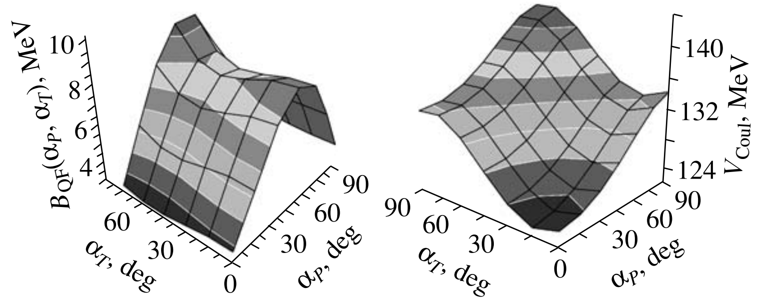

Fig. 5. The dependences of the depth (left panel) of the potential well (or quasifission barrier B_{QF}) and (right panel) of the Coulomb barrier (for $\ell = 0$) on the orientation angles of the projectile (α_P) and target (α_T) nuclei for the $^{48}Ca + ^{154}Sm$ reaction.

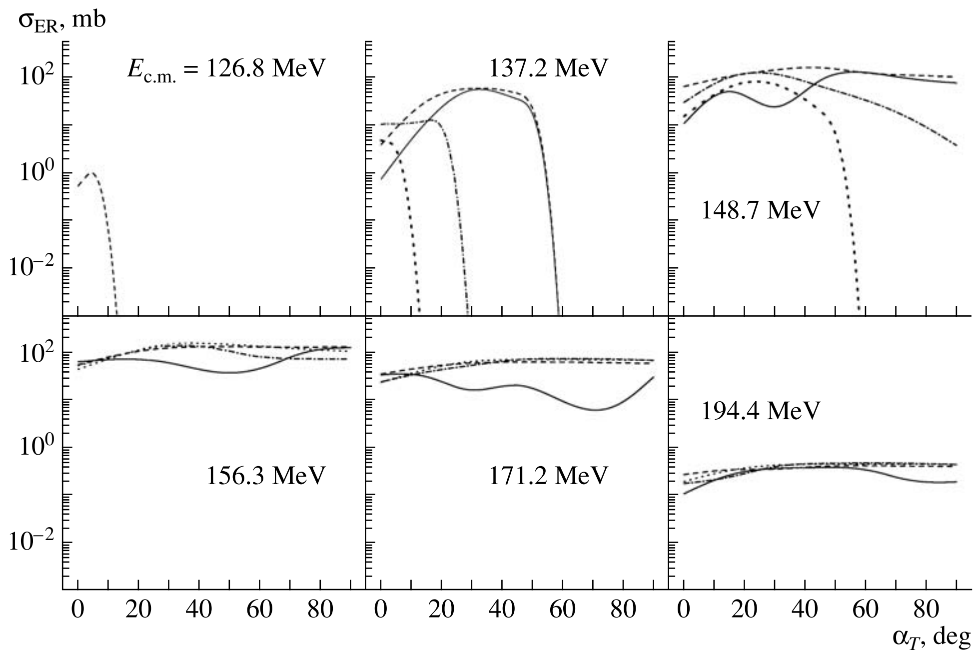

Fig. 6. Evaporation residue cross section versus the α_T orientation angle, at some fixed energies $E_{c.m.}$ and for a set of the α_P orientation angles for the $^{48}Ca + ^{154}Sm$ reaction: (solid curve) $\alpha_P = 0°$, (dashed curve) 30°, (dash-dotted curve) 60°, (dotted curve) 90°.

Deep potential well means the large quasifission barrier B_{QF} (left panel of Fig. 5). Our results showed that for these angles the intrinsic fusion barrier B_{fus} is small (Fig. 4) that creates favorable condition for complete fusion.

Due to the large Coulomb barrier V_{Coul} for the collisions with large orientation angles (right panel of Fig. 5) there is no contribution to fusion at low values of collision energy $E_{c.m.} < 140$ MeV. In collisions with the orientation angles $\alpha_P = 90°$ and $\alpha_T = 90°$, the compound nucleus is formed at large values of beam energy with large probability due to smallness of B_{fus}. In collisions with these orientation angles, the compound nucleus is formed only at large beam energies because the Coulomb barrier has large values for these orientation angles. This phenomenon was discussed in [5] and we observe it clearly for the investigated $^{48}Ca + ^{154}Sm$ reaction.

Calculations of dynamics of incoming paths show the following properties of the capture cross section:

(i) The capture of the projectile by the target nucleus takes place if the collision energy in the center-of-mass system is larger than the Coulomb barrier for the collision with corresponding orientation angles α_P and α_T.

(ii) The number of partial waves which determine the capture cross section increases by increasing the beam energy.

(iii) The number of partial waves is larger if the depth of the potential well is large.

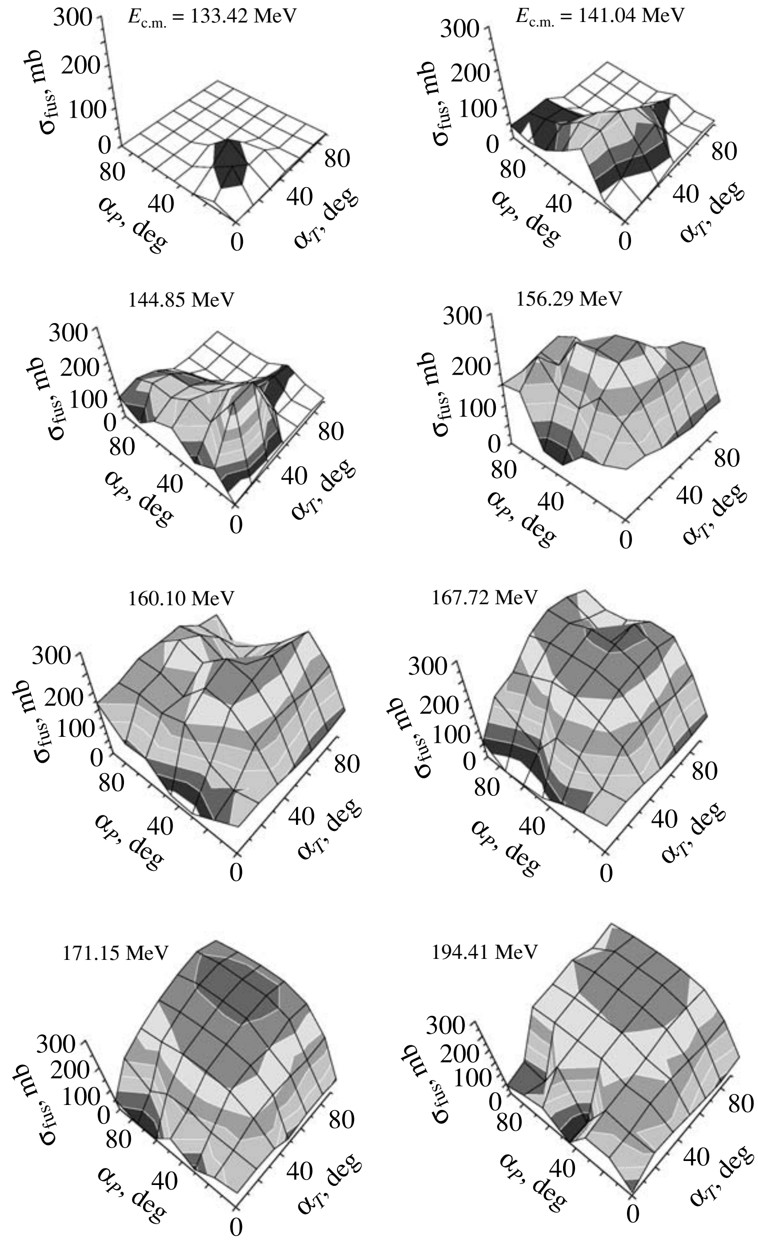

Fig. 7. Complete fusion cross section as a function of the orientation angles α_P and α_T for a set of fixed $E_{\mathrm{c.m.}}$ energy values.

(iv) The number of partial waves ceases to increase by increasing the beam energy for the given orientation angles α_P and α_T if the beam energy is larger enough than the Coulomb barrier due to the restricted value of the radial friction coefficient. So, for small values of the orbital angular momentum and large values of the beam energy we have a ℓ "window" because $\ell_{\min} > 0$. In fact, after dissipation of the relative kinetic energy the projectile could not be trapped into the potential well. The ℓ "window" properties may be inherent to all orientation angles of reactants [5].

At high energies the rate of the fusion formation at competition between quasifission and fusion increases. We note that the capture and fusion could occur in collisions with the large orientation angles of the reactants by increasing the beam energy. Moreover, at the high beam energies the number of partial waves ℓ also increases and the part of complete fusion going to fission of compound nucleus becomes comparable or larger than the cross section of the evaporation residue formation along the deexcitation cascade of the compound nuclei. In such a range of beam energies, due to the population of rotational states $\ell > \ell_f$ the contribution of the fast fission appears and becomes noticeable ($\ell_f = 82\hbar$ for ^{202}Pb). This phenomenon is seen from our results (see Fig. 2)

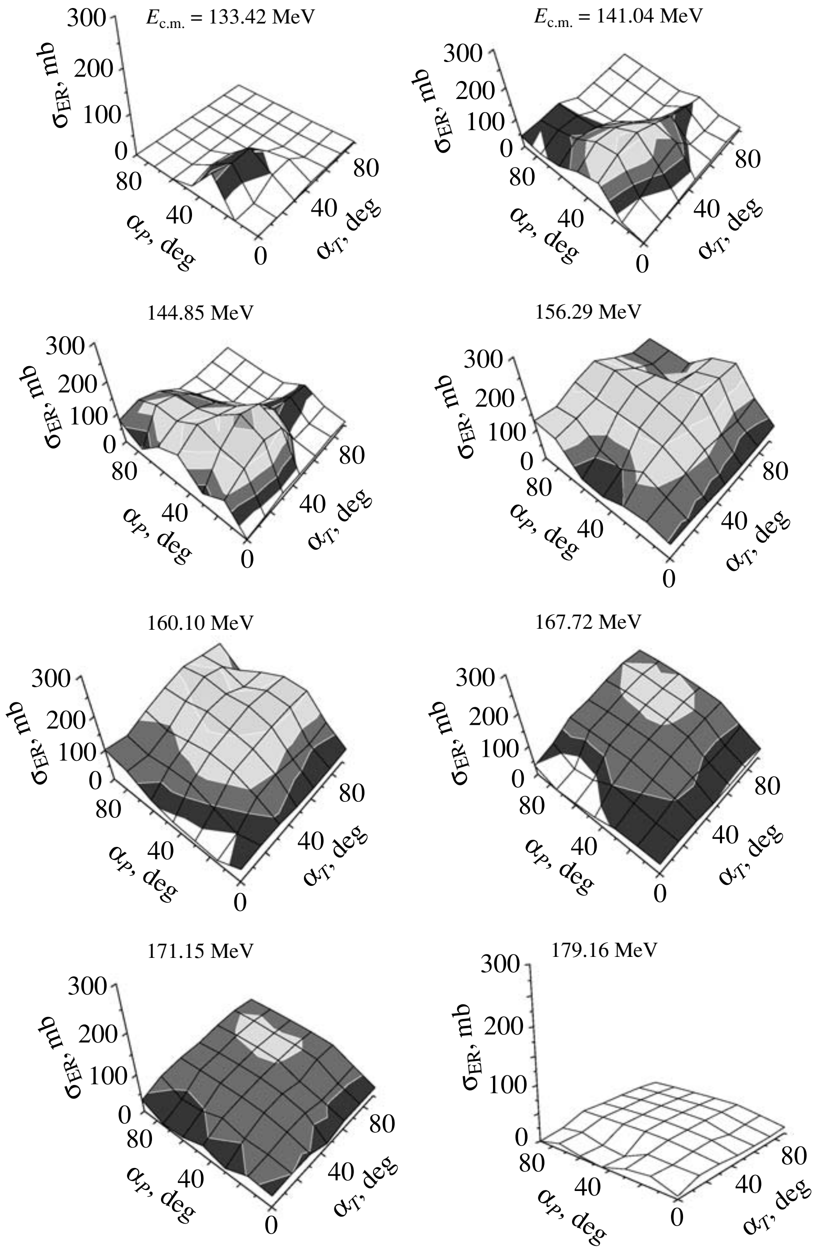

Fig. 8. Evaporation residue cross section as a function of the orientation angles α_P and α_T for a set of fixed $E_{c.m.}$ energy.

obtained for the complete fusion, quasifission, and fast fission events in the reaction under discussion.

The dependence of the production of the evaporation residue nuclei on the orientation angle α_T of the target–nucleus symmetry axis is presented in Fig. 6 for some values of the beam energy and orientation angle α_P of the projectile symmetry axis. In the figure, the different curves are related to various values of α_P. At the smallest beam energy $E_{c.m.} = 125.8$ MeV (corresponding to $E^*_{CN} = 35.1$ MeV) we observe the evaporation residue cross section only for $\alpha_P = 30°$ and the $\alpha_T = 0°–12°$ range. At $E_{c.m.} = 137.2$ MeV ($E^*_{CN} = 46.5$ MeV), the number of orientation angles giving contributions to the evaporation residue production increases and we obtain observable results for $\alpha_P = 0°$, $30°$, $60°$, $90°$ in the ranges of the α_T orientations from $0°$ up to $59°$, $58°$, $28°$, and $13°$, respectively, because in the collisions with these beam energies the capture and complete fusion are impossible for larger values of the orientation angles α_T. Therefore, when the beam energy is large enough (for example, $E_{c.m.} = 156.3$ MeV or $E_{c.m.} = 171.2$ MeV corresponding to $E^*_{CN} = 65.6$ or 80.8 MeV), all orientation angles of reactants lead to the observation of the evaporation residues with cross sections in the range 10–100 mb. At $E_{\rm c.m.} = 194.4$ MeV ($E^*_{\rm CN} = 103.7$ MeV) all orientation angles can contribute to form the evaporation residues, but with small cross sections, $\sigma_{\rm ER} = 1$–0.1 mb. Because by increasing the beam energy the number of partial waves leading to the complete fusion increases. The decrease of $\sigma_{\rm ER}$ at $E_{\rm c.m.} = 194.4$ MeV is connected with the fact that the fission barrier for a compound nucleus decreases by increasing its excitation energy [11, 17] and angular momentum [6]. Therefore, survival probability of the heated and rotating compound nucleus along deexcitation cascade decreases. Another phenomenon leading to the decrease of $\sigma_{\rm ER}$ at higher beam energy is the fast fission process which takes place if angular momentum of the being formed compound nucleus is larger than ℓ_f (see dash-double-dotted curve in Fig. 2).

In Fig. 7 the dependence of the fusion cross section $\sigma_{\rm fus}$ on the orientation angles of interacting nuclei is presented for different values of $E_{\rm c.m.}$. At low values of $E_{\rm c.m.}$ small values of the orientation angles α_P and α_T can only contribute to $\sigma_{\rm fus}$. At large $E_{\rm c.m.}$ values the large orientation angles α_P and α_T start to contribute to the fusion cross section, while the contribution of the small orientation angles α_P and α_T to $\sigma_{\rm fus}$ decreases. It is connected by appearing of ℓ window in capture.

At last, Fig. 8 shows the evaporation residue production as a function of orientation angles α_P and α_T at moment of the DNS formation. This dependence is connected with the angular momentum distribution $\sigma^{(\ell)}_{\rm fus}$ of the compound nucleus (Fig. 3) because the survival probability of the heated and rotating compound nucleus depends not only on excitation energy but on its angular momentum too. It was widely presented and discussed in [11]. Certainly, at low $E_{\rm c.m.}$ noticeable evaporation residue cross section can be observed only for collisions with small values α_P and α_T. At $E_{\rm c.m.} = 150$–160 MeV the evaporation residue yields reach the remarkable contributions for large α_P and α_T angles, and at $E_{\rm c.m.} > 170$ MeV the evaporation residue production is contributed by the large α_P–α_T configurations, but the evaporation residue yield is strongly reduced due to the intense fission process.

3. CONCLUSIONS

The role of the orientation angles α_P and α_T of the symmetry axes of reacting nuclei in the complete fusion and evaporation residue cross sections is studied for the ^{48}Ca + ^{154}Sm reaction at near and above Coulomb barrier energies. The dependencies of the quasifission–fusion competition during the evolution of the dinuclear system and the sensitivity of the fission–evaporation competition during the deexcitation cascade of the compound nucleus on the values of orientation angles α_P and α_T are demonstrated. The analysis of the dependence of the compound nucleus and evaporation residue formation cross sections on the orientation angles α_P and α_T of the reacting nuclei showed that the observed yield of evaporation residues in the ^{48}Ca + ^{154}Sm reaction at low beam energies ($E_{\rm c.m.} < 133$ MeV) is formed in the collisions with small low orientation angles (about $\alpha_P = 30^\circ$ and $\alpha_T = 0^\circ$–12°). Because a collision with the given orientation angles α_P and α_T can contribute to formation of evaporation residues if the beam energy is enough to overcome the corresponding Coulomb barrier. Only in this case it is possible formation of dinuclear system which evolves to compound nucleus or breaks up into two fragments after multinucleon exchange without formation of the compound nucleus. At more large beam energies (about $E_{\rm c.m.} = 140$–180 MeV) all α_P–α_T orientation angles of reactants can contribute to $\sigma_{\rm ER}$ and its values are in the 10–100-mb range. At more large beam energies, at $E_{\rm c.m.} > 185$ MeV, the complete fusion increases (see Fig. 3), but the evaporation residue cross section $\sigma_{\rm ER}$ goes down and its values are in the 1–0.1-mb range due to the strong decrease of the survival probability of the heated compound nucleus along deexcitation cascade. This is connected by the decrease of the fission barrier for a compound nucleus by increasing its excitation energy [16, 17] and angular momentum [6].

Another phenomenon leading to decrease of $\sigma_{\rm ER}$ at more high beam energy is the fast-fission process which is the splitting of the mononucleus into two fragments due to absence of the fission barrier at very high angular momentum $\ell > \ell_f$, where ℓ_f is the value of angular momentum at which barrier disappears.

ACKNOWLEDGMENTS

G. Giardina and A.K. Nasirov are grateful to the Fondazione Bonino-Pulejo (FBP) of Messina for the important support received in the international collaboration between the Messina group and the Joint Institute for Nuclear Research of Dubna (Russia). A.K. Nasirov thanks DFG and RFBR for partial support.

REFERENCES

1. S. Hofmann and G. Munzenberg, Rev. Mod. Phys. **72**, 733 (2000).
2. K. Morita et al., J. Phys. Soc. Jpn. **73**, 2593 (2004).
3. Yu. Ts. Oganessian et al., Phys. Rev. C **70**, 064609 (2004).
4. K. Nishio et al., Eur. Phys. J. A **29**, 281 (2006).

5. A. K. Nasirov et al., Nucl. Phys. A **759**, 342 (2005).
6. A. J. Sierk, Phys. Rev. C **33**, 2039 (1986).
7. A. M. Stefanini et al., Eur. Phys. J. A **23**, 473 (2005).
8. G. Giardina et al., Eur. Phys. J. A **8**, 205 (2000).
9. G. Giardina et al., Nucl. Phys. A **671**, 165 (2000).
10. G. G. Adamian et al., Nucl. Phys. A **633**, 409c (1998).
11. G. Fazio et al., Eur. Phys. J. A **22**, 75 (2004).
12. A. K. Nasirov et al., in *Proc. of the Symp. on Nuclear Cluster, Rauischolzhausen, Germany, 2002*, Ed. by R. V. Jolos and W. Scheid (EP Systema, Debrecen, 2003), p. 415; A. K. Nasirov et al., Acta Phys. Hung. A **19**, 109 (2004).
13. G. Audi and A. H. Wapstra, Nucl. Phys. A **595**, 409 (1995).
14. P. Moller, J. R. Nix, W. D. Myers, and W. J. Swiatecki, At. Data Nucl. Data Tables **59**, 185 (1995).
15. G. Fazio et al., Mod. Phys. Lett. A **20**, 391 (2005).
16. G. Fazio et al., Eur. Phys. J. A **19**, 89 (2004).
17. G. Fazio et al., J. Phys. Soc. Jpn. **72**, 2509 (2003).
18. A. K. Nasirov et al., Eur. Phys. J. A **34**, 325 (2007).
19. A. D'Arrigo et al., J. Phys. G **20**, 365 (1994).
20. A. D'Arrigo et al., Phys. Rev. C **46**, 1437 (1992).
21. S. Raman et al., At. Data Nucl. Data Tables **36**, 1 (1987).
22. R. H. Spear, At. Data Nucl. Data Tables **42**, 55 (1989).
23. D. J. Hinde et al., Phys. Rev. C **53**, 1290 (1996).
24. G. Fazio et al., Phys. Rev. C **72**, 064614 (2005).